Pergamon

Bioorganic & Medicinal Chemistry 8 (2000) 1599–1605

BIOORGANIC & MEDICINAL CHEMISTRY

Hydrogen Bonding Isosteres: Bimolecular Carboxylic Acid and Amine-*N*-oxide Interactions Mediated Via CH···O Hydrogen Bonds

P. W. Baures,* A. Wiznycia and A. M. Beatty

Department of Chemistry, Kansas State University, Manhattan, KS 66506, USA

Received 15 October 1999; accepted 6 March 2000

Abstract—The X-ray structures of cocrystals between 2,2′-dipyridyl-*N*,*N*′-dioxide (**1**) with fumaric acid (**2**), itaconic acid (**3**), succinic acid (**4**), and oxalic acid (**5**) were solved to determine if concurrent CH···O interactions were capable of orienting the bimolecular association of the two molecules. Cocrystals **1·2**, **1·3** and **1·4** produce cyclic hydrogen bonded motifs employing pair-wise OH···O and CH···O hydrogen bonds, whereas cocrystal **1·5** forms analogous OH···O hydrogen bonds with a different set of intermolecular CH···O hydrogen bonds. Evidence of cocrystal formation was also observed for these complexes by differential scanning calorimetry and FT-IR spectroscopy. The structures of **1·2**, **1·3** and **1·4** demonstrate the potential of the pair-wise OH···O and CH···O hydrogen bonding interactions and serve to illustrate their use as hydrogen bonding isosteres in crystal engineering, molecular recognition, and drug design.

Introduction

Chemists often include traditional hydrogen bond donors and acceptors into drug candidates when trying to create particular hydrogen bonding contacts (OH···O, NH···O, OH···N, or NH···N) within a macromolecular binding site.[1] Crystal engineers have similarly constructed supramolecular assemblies by employing strong hydrogen bonds;[2] however, they have also utilized weaker intermolecular forces such as CH···O,[3] CH···N,[4] or halogen···halogen[5] interactions in the design of new materials. The importance of CH···O interactions in biological systems is under continuing investigation[6] and chemists in the future may routinely consider these interactions as a way to provide greater diversity in the structures and associated properties of candidate drug compounds.

Our initial objective has been to identify functional groups which form predictable CH···O hydrogen bonding interactions with themselves or with other functional groups as a prelude to incorporating these interactions into potentially bioactive compounds. Amine-*N*-oxides are strong hydrogen bond acceptors[7] and complexes of amine-*N*-oxides with carboxylic acids have been previously characterized in solution.[8] Structural details of these intermolecular interactions can be found by examining the relevant X-ray structures of cocrystalline aromatic amine-*N*-oxides with carboxylic acids, which show the formation of a cyclic hydrogen-bonded motif formed by pair-wise OH···O and CH···O hydrogen bonds.[9]

Similar bimolecular interactions in the solid-state involving only strong hydrogen bonding contacts (OH···O, NH···O, OH···N, or NH···N) have been identified and examined,[10] although increasing attention is being given to weaker non-covalent interactions.[11] The cyclic hydrogen bonding motifs commonly formed in the solution aggregation and solid-state organization of carboxylic acids and cyclic amides are well known[12] (Fig. 1, *A* and *B* respectively), forming $R_2^2(8)$ motifs.[13] Furthermore, it is known that mixtures of carboxylic acids and amides will often aggregate to form acid–amide dimers, *D*, specifically on the basis of this cyclic hydrogen bonded motif.[14] The utility of isographic hydrogen bonding patterns, meaning those which mimic one another in terms of hydrogen bond donor and acceptor interactions, has previously been shown to be useful in designing new solids and in comparing known solid-state structures.[15] In fact, even relatively weak CH···O hydrogen bonds participate in forming cyclic dimers in aromatic amine-*N*-oxides (*C*), resulting in complexes isographic to the acid dimers, the amide dimers, or the acid–amide dimers, and have recently been utilized for supramolecular assembly.[16]

*Corresponding author. Tel.: +1-785-532-6665; fax: +1-785-532-6666; e-mail: baures@ksu.edu

0968-0896/00/$ - see front matter
PII: S0968-0896(00)00090-0

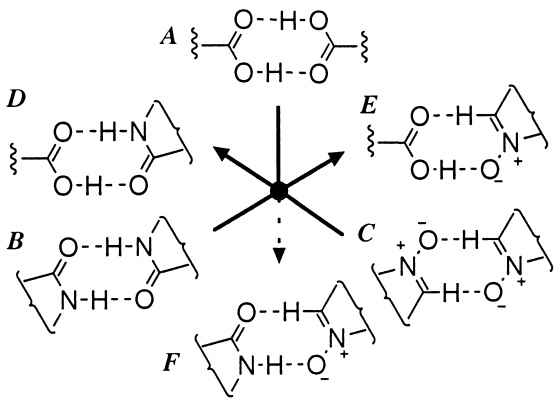

Figure 1. Hydrogen bond diagram illustrating the isographic nature of the bimolecular pair-wise association of carboxylic acids, amides, and aromatic amine-*N*-oxides. The lines illustrate the unimolecular association of these functional groups, whereas the arrows describe mixed functional group associations. The amide with amine-*N*-oxide combination has not been researched to date as noted by the dashed arrow.

The present study was undertaken in an effort to better understand the molecular aggregates formed between carboxylic acids and amine-*N*-oxides (*E*). Furthermore, it was of interest to determine whether these molecular aggregates are isographic to the other well-known cyclic dimers previously mentioned (*A*, *B*, and *D*), since this would infer that the groups may potentially substitute for one another in crystal engineering, molecular recognition, or drug design projects. Although complexes of amine-*N*-oxides and carboxylic acids have been extensively studied in solution,[8] only a few crystal structures exist in the Cambridge Crystallographic Data File (CCDF, Version 5.17, April 1999) which could potentially form this cyclic hydrogen bonded motif. Of these X-ray structures, most are organized by the pair-wise intermolecular motif *E* (Fig. 1),[9a–e] while others do not form this interaction.[17] Only a functional group position is different between a structure forming this bimolecular motif and the structure which does not form this motif, which exemplifies the need to further explore the reliability of this interaction. Another cocrystalline pair-wise hydrogen bonded complex with this motif (*E*) has been reported since this version of the CCDF was distributed.[9f]

This work identifies and characterizes 1:1 cocrystalline structures between 2,2′-dipyridyl-*N*,*N*′-dioxide and fumaric acid (**1·2**), 2,2′-dipyridyl-*N*,*N*′-dioxide and itaconic acid (**1·3**), 2,2′-dipyridyl-*N*,*N*′-dioxide and succinic acid (**1·4**), as well as 2,2′-dipyridyl-*N*,*N*′-dioxide and oxalic acid (**1·5**). Compound **1** was chosen for this initial study because it has only one *ortho* CH group next to each *N*-oxide functionality, forms crystals under ambient conditions, is uncomplicated by other common functional groups, and is readily available. Solid materials were obtained by preparing aqueous solutions of **1** mixed with simple dicarboxylic acids, allowing the water to evaporate, and analyzing the materials by using differential scanning calorimetry, FT-IR spectroscopy, and single-crystal X-ray diffraction.

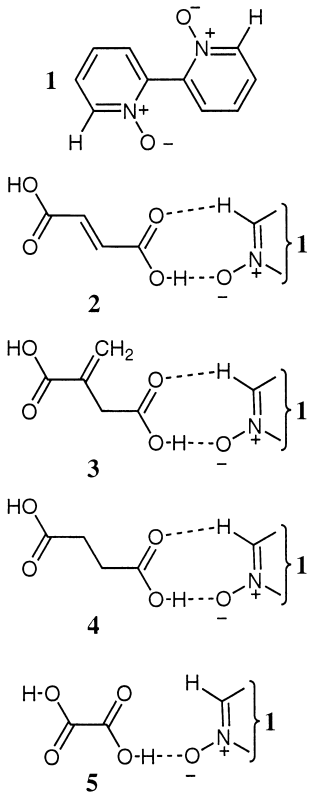

Results

Differential scanning calorimetry

The melting points of the solids obtained were first analyzed to determine if a new material had been formed. In most cases, heating the samples resulted in decomposition or sublimation or both. The initial temperature of these transitions is difficult to observe with certainty; thus, we chose to also measure the behavior of the solids by differential scanning calorimetry. These determinations were only qualitative because the changes are irreversible due to the aforementioned decomposition or sublimation. Nevertheless, the DSC data do support cocrystallization due to the distinct thermal transitions of the mixed solids as compared to the starting materials.[18]

FT-IR spectroscopy

Preliminary evidence of cocrystallization was also sought by comparison of the solid-state FT-IR spectra of the individual components with those of solids obtained from solutions containing both components. The purpose of FT-IR analysis was to compare the stretching frequencies of the carboxylic acid and amine-*N*-oxide functional groups in the potential complex as an indication of whether they were involved in hydrogen bond interactions different than those they normally form in the pure substances. For example, the significant absorbances for the carboxylic acid and amine-*N*-oxide functional groups as observed in the solids examined in this study are given in Table 1. There are changes in each of the two regions which can be

Table 1. Infra-red stretching frequencies for the carboxylic acid and amine-*N*-oxide groups[a]

Sample[b]	C=O (1750–1650 cm^{-1})		C–O, N–O (1270–1200 cm^{-1})	
	KBr	Fluorolube	KBr	Fluorolube
2,2′-Dipyridyl-*N*,*N*′-dioxide (**1**)	[c]	[c]	*1268*, 1262, 1255, (1250)	*1268*, 1263, 1256, (1250)
Fumaric acid (**2**)	1675	1677	1232, *1214*	1232, *1214*
1·2	1693	1693	1236, 1227, 1208	1237, 1222, 1208
Itaconic acid (**3**)	1704	1706	*1231*, 1216	(1231), 1216
1·3	1711, 1690	1711, 1690	1242, 1234, 1219	1243, 1234, *1223*
Succinic acid (**4**)	1694	1697	*1214*, 1209	*1213*, 1203
1·4	1699	1699	1268, (1252), 1238, 1225, (1217)	1268, (1263), (1252), 1238, 1226, (1217)
Oxalic acid (**5**)	1688	1685	1254[d]	1253[d], (1232)
1·5	1702	1697	1265, 1237	1265, 1236

[a]Italicized frequencies are observed to be of modest relative intensity (20–50%) to comparable absorption bands in the same spectrum, whereas, frequencies enclosed in parentheses are shoulders or relatively weak absorption bands (< 20%).
[b]Preparation is further described in Experimental.
[c]This region is absorption free.
[d]Very broad absorption band (~1280–1210 cm^{-1}).

attributed to cocrystal formation. The C=O stretch is shifted from 1677 cm^{-1} in **2** to a maximum of 1693 cm^{-1} in **1·2**, consistent with hydrogen bond complexation between the carboxylic acid and amine-*N*-oxide. The C–O and N–O stretching region is less useful due to the presence of multiple overlapping absorption bands, but the observed differences are themselves diagnostic of novel solid-state structure. The absorption bands for the carbonyl group in the 1:1 cocrystals are found at 1693 cm^{-1} for **1·2**, 1690 and 1711 cm^{-1} for **1·3**, 1699 cm^{-1} for **1·4**, and either 1702 or 1697 cm^{-1} in KBr and fluorolube, respectively, for **1·5**. The two absorption bands for the carbonyl group in the **1·3** cocrystal are likely a difference in the environment between the two dissimilar carboxylic acids, since both interact similarly in their intermolecular hydrogen bonding patterns. In the N–O and C–O stretching region, cocrystal formation is indicated in KBr samples by the loss or reduction of the amine-*N*-oxide absorption bands at 1262 cm^{-1} and 1255 cm^{-1}, with new absorption bands found at 1236 cm^{-1} in **1·2**, 1242 and 1234 cm^{-1} in **1·3**, 1238 cm^{-1} in **1·4**, and at 1237 cm^{-1} in **1·5**. It is important to note that in **3** alone there are also absorption bands at 1242 and 1234 cm^{-1}, but the relative strengths of these bands is different in the 1:1 cocrystal coinciding with the loss of the amine-*N*-oxide stretches at 1262 and 1255 cm^{-1}. In general, there are few differences between the FT-IR spectrum of **1·2** compared with those obtained for **1·3**, **1·4** and **1·5**, or between the spectra measured in fluorolube versus those collected as KBr pellets.

X-ray crystallography

Single crystals of **1·2**, **1·3**, **1·4** and **1·5** were used for X-ray diffraction analysis in order to clearly identify the interactions involved in the bimolecular association. The molecular structures of the cocrystals do not display any unusual structural characteristics (bond lengths or angles). The molecular representations for the X-ray crystal structures of **1·2**, **1·3**, **1·4** and **1·5** are shown in Figures 2–5, respectively, along with the crystallographically defined atom labels for the asymmetric unit in each crystal structure. Comparative crystallographic information for the cocrystals is given in Table 2.

Hydrogen bonds between the carboxylic acid and amine-*N*-oxide functional groups are responsible for the bimolecular association of the individual molecules in each of the four cocrystalline structures. Hydrogen bond distance and angle information for the bimolecular association contacts in the X-ray structures is supplied in Table 3. The relative orientation of the individual molecules in **1·2**, **1·3** and **1·4** is controlled by concurrent formation of an intermolecular CH···O hydrogen bond between the *ortho* C-H of **1** with a carboxylic acid carbonyl oxygen of the diacid. The cocrystal structure of **1·5** does not contain the same pair-wise hydrogen bonding arrangement observed in the other structures, despite the strong OH···O interactions between the unique oxalic acid and amine-*N*-oxide molecules. A unit cell packing diagram is shown in Figure 6 for this cocrystal.

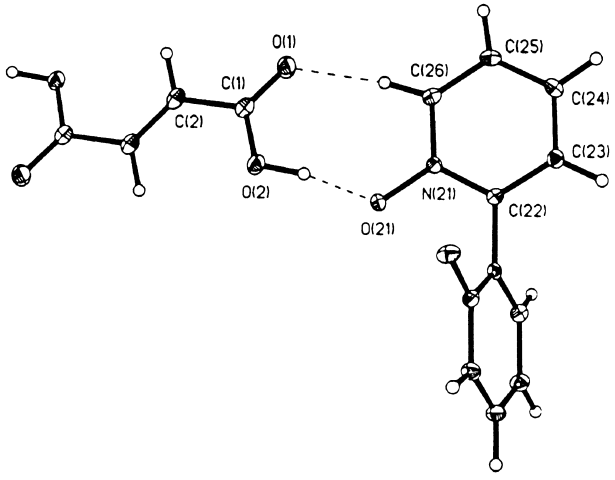

Figure 2. X-ray crystal structure for **1·2** and the atom labeling scheme (30% thermal ellipsoids). Only those atoms in the asymmetric unit are labeled.

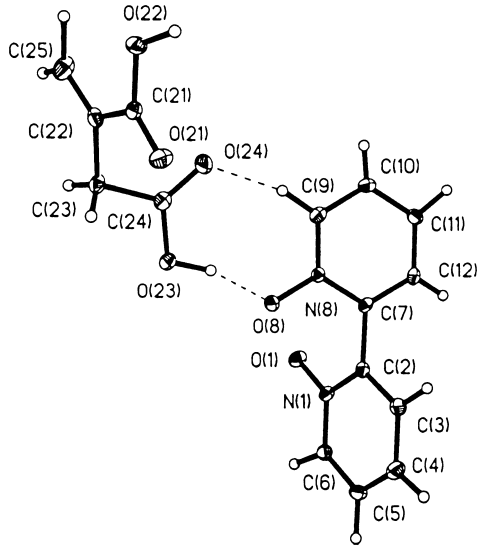

Figure 3. X-ray crystal structure for **1·3** and the atom labeling scheme (30% thermal ellipsoids).

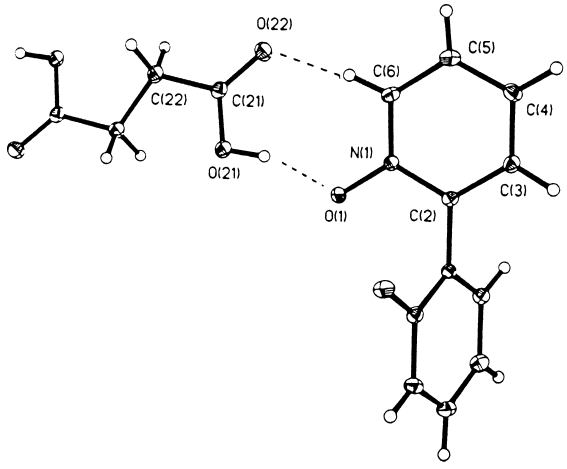

Figure 4. X-ray crystal structure for **1·4** and the atom labeling scheme (30% thermal ellipsoids). Only those atoms in the asymmetric unit are labeled.

Discussion

The X-ray crystal structures of **1·2**, **1·3**, **1·4** and **1·5** were determined in order to examine the bimolecular associations in greater detail, showing that **1·2**, **1·3** and **1·4** exhibit the anticipated $R_2^2(8)$ motif[13] formed by a pair-wise strong OH···O hydrogen bond coupled with a weaker CH···O hydrogen bond. The structure of **1·5** is not organized via pair-wise hydrogen bonding interactions but does retain an OH···O hydrogen bond between **5** and **1,** respectively. The reason **1·5** does not form the anticipated hydrogen bonding motif is not entirely clear, although the similarity in size between **5** and one half of **1** may be responsible for this alteration (Fig. 6). It may be argued that the formation of the bimolecular pair-wise arrangement and resulting CH···O contacts observed in **1·2**, **1·3** and **1·4** were induced by crystallization, thereby suggesting that these X-ray structures do not represent the most energetically favorable arrangement between these two functional groups in solution. However, binding sites in receptors or active sites in enzymes are also

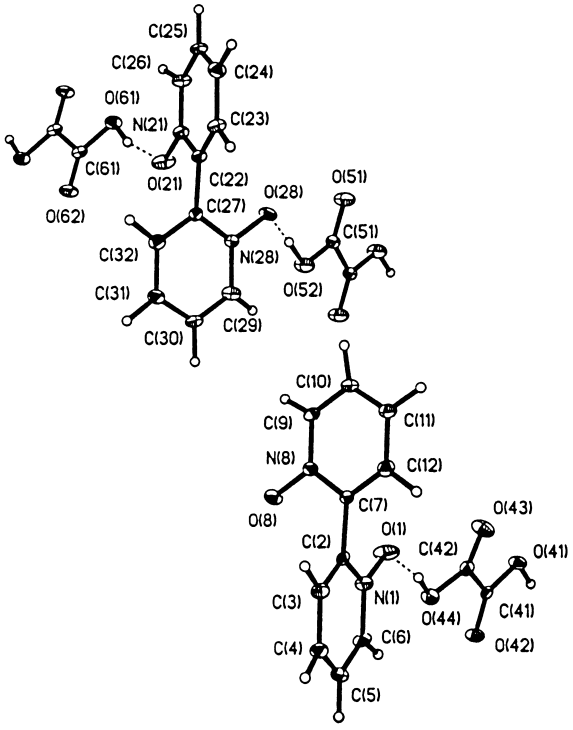

Figure 5. X-ray crystal structure for **1·5** and the atom labeling scheme (30% thermal ellipsoids). Only those atoms in the asymmetric unit are labeled.

constraining and contextual; that is, these sites present distinct complementarities to limit what molecules may bind to them. In each case, an appropriate combination of size, shape, electronic, and hydrophobic complementarity to the macromolecular site must be met which results in overall stabilization of the binding interaction.

The DSC analysis and FT-IR spectra provided an indication of cocrystal formation for the 1:1 molecular and functional group stoichiometries, and are therefore useful in identifying complexation. The infrared data do not indicate per se the hydrogen bond motif formed between the amine-*N*-oxide and carboxylic acid in the cocrystalline solids, despite clear qualitative differences between these spectra and those of simply the amine-*N*-oxide or dicarboxylic acids.

The potential of non-traditional changes in drug design is illustrated by considering three of the known thermolysin inhibitors. These structures and the reported inhibition constants are compared in Figure 7.[19] The phosphonates bound to the active site with a reduction of 4.0 kcal/mol in binding affinity compared to the phosphonamidates. Interestingly, the phosphinates bound with only a 0.1 kcal/mol reduction in binding affinity, attributed to differences not only in the active site interactions formed between inhibitor and enzyme, but also the weaker solvent interactions disrupted in desolvation prior to the binding step. Similar enthalpy/entropy compensations are presented as an explanation of agonist, partial agonist, and antagonist activity in receptor binding, as well as the importance of host–guest interactions.[20]

Table 2. Selected data collection and refinement data for **1·2**, **1·3**, **1·4** and **1·5**

Crystal data	**1·2**	**1·3**	**1·4**	**1·5**
Crystal size (mm)	0.50×0.30×0.20	0.42×0.28×0.18	0.48×0.28×0.18	0.30×0.30×0.20
Crystal system	Monoclinic	Orthorhombic	Monoclinic	Monoclinic
Space group	C2/c	$P2_12_12_1$	C2/c	$P2_1/c$
a (Å)	12.596(1)	5.247(1)	12.595(1)	13.439(1)
b (Å)	5.159(3)	11.516(1)	5.329(1)	10.965(1)
c (Å)	19.725(1)	24.283(3)	20.290(2)	16.628(2)
α (°)	90.0	90.0	90.0	90.0
β (°	98.08(1)	90.0	100.31(1)	104.43(1)
γ (°)	90.0	90.0	90.0	90.0
R/R_w^2 (obs. data)	0.0318/0.0757	0.0488/0.1019	0.0415/0.1142	0.0507/0.1066
$\Delta\rho_{max/min}$ (e Å^{-3})	0.180/−0.226	0.235/−0.265	0.423/−0.329	0.175/−0.269
S	1.083	1.020	1.066	1.002

Table 3. Geometric information for selected hydrogen bonds in cocrystals **1·2**, **1·3**, **1·4** and **1·5**

X-ray	Contact	D···A (Å)	D–H···A ∠ (°)
1·2	O2–H···O21A	2.584(1)	168(1)
	C26–H···O1	3.200(1)	170(1)
1·3	O23–H···O8	2.551(1)	157(1)
	C9–H···O24	3.332(1)	156(1)
	O22–H···O1A	2.628(1)	164(1)
	C6A–H···O21	3.164(1)	157(1)
1·4	O21–H···O1	2.612(1)	163(1)
	C6–H···O22	3.203(1)	159(1)
1·5	O44–H···O1	2.491(1)	162(1)
	O41–H···O8	2.501(1)	167(1)
	O52–H···O28	2.496(1)	177(1)
	O61–H···O21	2.516(1)	167(1)

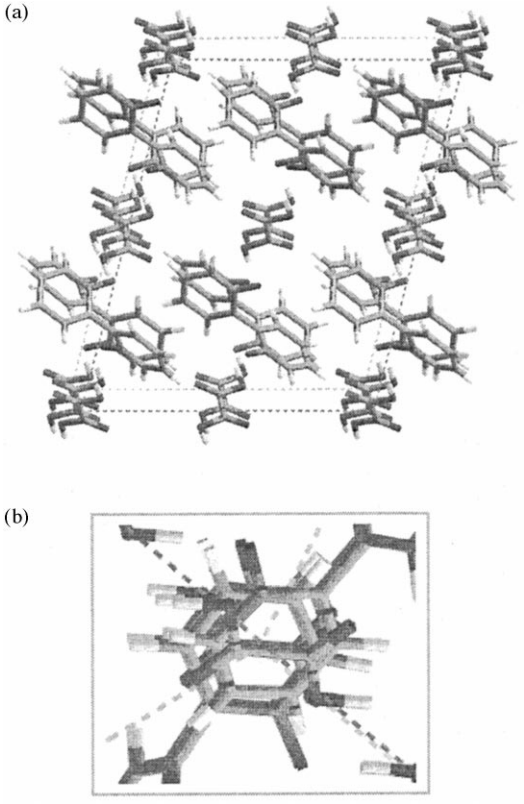

Figure 6. (a) X-ray crystal structure packing diagram for **1·5** viewed down the *b* axis. (b) This view is looking through the unit cell from the lower left to the upper right (down the [121] axis) indicating the superpositioning of **5** with two halves of **1** in a repetitive fashion.

Conclusion

The dimeric association of a carboxylic acid with an aromatic amine-*N*-oxide functional group can be controlled in part by the concurrent formation of intermolecular CH···O interactions in the assembly. The resulting hydrogen bonding motifs are isographic to well known cyclic dimers which are important in crystal engineering, molecular recognition, and drug design research. In that context, the work described herein aims to help recognize isographic hydrogen bonding interactions which may be underutilized and find use in these research areas.

Experimental

General cocrystal formation: preparation of 1·4

Into a small glass vial was weighed 9.4 mg (0.5×10^{-4} mol) of 2,2′-dipyridyl-*N*,*N*′-dioxide (**1**) and 4.5 mg (0.5×10^{-4} mol) of oxalic acid (**5**), to which 2.0 mL of H_2O was added. Solutions of **1** and of **5** were similarly prepared as controls. The solutions were kept at room temperature in a dust free environment until all the water had fully evaporated (3–5 days). The solutions of fumaric acid (**2**), itaconic acid (**3**) and succinic acid (**4**) were prepared analogously. The resulting solids left after evaporation were examined for possible X-ray quality crystals, of which a small number were removed. The remaining solid was briefly pulverized and a representative sample was used for subseqent DSC analysis and FT-IR spectroscopy.

Differential scanning calorimetry analysis. Solids were analyzed by using a Perkin–Elmer Pyris-1. Samples were sealed in aluminum pans and heated at a rate of 20 °C/min from room temperature to 320 °C, measuring the thermal transitions relative to an empty reference pan.[18]

FT-IR solid-phase analysis. Spectra were collected with a Nicolet Protégé 460 spectrometer. Spectra were collected at 1 cm^{-1} resolution on the solids from the complexation

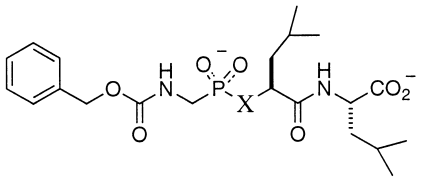

X	K_i (nM)
NH	9.1
O	9000
CH	10.6

Figure 7. Thermolysin inhibitor structures and their inhibitor constants.

experiments in both fluorolube on NaCl plates as well as by the preparation of KBr pellets. A total of 32 scans were averaged. For fluorolube samples, a background sample of fluorolube was run before every sample then a small quantity of a concentrated mulled sample in fluorolube was added between the sodium chloride plates to obtain the sample spectra. This method produced higher quality spectra than did spectral subtraction of the fluorolube.

X-ray single-crystal diffraction. The crystal data for **1·2**, **1·3** and **1·4** were collected by using a Siemens P4 four-circle diffractometer with graphite monochromated Mo-K_α ($\lambda = 0.71073$ Å) radiation at -100 °C. Crystal stabilities were monitored by measuring three standard reflections after every 97 reflections with no significant decay in observed intensities. A θ–2θ scanning technique was used for peak collection with Lorenz and polarization corrections applied. Hydrogen atom positions were located from difference Fourier maps and a riding model with fixed thermal parameters ($u_{ij} = 1.2U_{ij}$(equiv) for the atom to which they are bonded) was used for subsequent refinements. The weighting function applied was $w^{-1} = [\sigma^2(F_o^2) + (g_1P)^2 + (g_2P)]$ where $P = [F_o^2 + 2F_c^2]/3$. The data for **1·5** were collected with a Bruker SMART 1000 CCD and integrated using SAINT. In all structures the SHELXTL PC and SHELXL-93 packages[21] were used for data reduction, structure solution, and refinement.[22]

Acknowledgements

This material is based upon the work supported by the National Science Foundation under Grant No. EPS-9550487 and matching support from the state of Kansas. The financial support of the Department of Chemistry at Kansas State University is also greatly appreciated. The authors would like to thank Christer B. Aakeröy for helpful discussions and comments.

References and Notes

1. For examples of structure-based drug design and hydrogen bond considerations, see: (a) Hubbard, R. E. *Curr. Opin. Biotechnol.* **1997**, *8*, 696. (b) Babine, R. E.; Bender, S. L. *Chem. Rev.* **1997**, *97*, 1359. (c) Wlodawer, A.; Vondrasek, J. *Annu. Rev. Biophys. Biomol. Struct.* **1998**, *27*, 249. (d) Aakeröy, C. B. In *Crystal Engineering*; Seddon, K. R.; Zaworotko, M., Eds.; Kluwer Academic Publishers: Dordrecht, The Netherlands, 1999; pp 303–324.
2. (a) Aakeröy, C. B.; Seddon, K. R. *Chem. Soc. Rev.* **1993**, 397. (b) Desiraju, G. R. *Angew. Chem., Int. Ed. Engl.* **1995**, *34*, 2311. (c) Aakeröy, C. B. *Acta Cryst.* **1997**, *B53*, 569.
3. (a) Sarma, J. A. R. P.; Desiraju, G. R. *Acc. Chem. Res.* **1986**, *19*, 222. (b) Desiraju, G. R. *Acc. Chem. Res.* **1991**, *24*, 290. (c) Krishnamohan Sharma, C. V.; Panneerselvam, K.; Pilati, T.; Desiraju, G. R. *J. Chem. Soc. Chem. Commun.* **1992**, 832. (d) Biradha, K.; Krishnamohan Sharma, C. V.; Panneerselvam, K.; Shimoni, L.; Carrell, H. L.; Zacharias, D. E.; Desiraju, G. R. *J. Chem. Soc. Chem. Commun.* **1993**, 1473. (e) Sarma, J. A. R. P.; Desiraju, G. R. *Acc. Chem. Res.* **1996**, *29*, 441; (f) Steiner, T. *Cryst. Rev.* **1996**, *6*, 1. (g) Carrell, H. L.; Glusker, J. P. *Structural Chemistry* **1997**, *8*, 141. (h) Anthony, A.; Desiraju, G. R.; Jetti, R. K. R.; Kuduva, S. S.; Madhavi, N. N. L.; Nangia, A.; Thaimattam, R.; Thalladi, V. R. *Crystal Engineering* **1998**, *1*, 1.
4. Marjo, C. E.; Scudder, M. L.; Craig, D. C.; Bishop, R. *J. Chem. Soc. Perkin Trans. 2* **1997**, 2099.
5. Navon, O.; Bernstein, J.; Khodorkovsky, V. *Angew. Chem., Int. Ed. Engl.* **1997**, *36*, 601.
6. (a) Pascard, C. *Acta Cryst.* **1995**, *D51*, 407. (b) Glusker, J. P. *Acta Cryst.* **1995**, *D51*, 418. (c) Derewenda, Z. S.; Lee, L.; Derewenda, U. *J. Mol. Biol.* **1995**, *252*, 248. (d) Whitesides, G. M.; Simanek, E. E.; Mathias, J. P.; Seto, C. T.; Chin, D. N.; Mammen, M.; Gordon, D. M. *Acc. Chem. Res.* **1995**, *28*, 37. (e) Leonard, G. A.; McAuley-Hecht, K.; Brown, T.; Hunter, W. *Acta Cryst.* **1995**, *D51*, 136. (f) Scrutton, N. S.; Raine, A. R. *Biochem. J.* **1996**, *319*, 1. (g) Engh, R. A.; Brandstetter, H.; Sucher, G.; Eichinger, A.; Baumann, U.; Bode, W.; Huber, R.; Poll, T.; Rudolph, R.; von der Saal, W. *Structure* **1996**, *4*, 1353. (h) Mandel-Gutfreund, Y.; Margalit, H.; Zhurkin, V. B. *J. Mol. Biol.* **1998**, *277*, 1129.
7. Taft, R. W.; Shuely, W. J.; Doherty, R. M.; Kamlet, M. J. *J. Org. Chem.* **1988**, *53*, 1737.
8. Dega-Szafran, Z.; Szafran, M. *J. Am. Chem. Soc.* **1994**, *37*, 627.
9. (a) Gorres, B. T.; McAfee, E. R.; Jacobson, R. A. *Acta Cryst.* **1975**, *B31*, 158. (b) Fuquen, R. M.; Lechat, J. R.; De Almeida Santos, R. H. *Acta Cryst.* **1991**, *C47*, 2388. (c) Moreno-Fuquen, R.; De Almeida Santos, R. H.; Gambardella, M. T. de P. *Acta Cryst.* **1997**, *C54*, 1634. (d) Moreno-Fuquen, R.; Grajales-Tamayo, M.; Gambardella, M. T. de P. *Acta Cryst.* **1997**, *C54*, 1635. (e) Moreno-Fuquen, R.; De Almeida Santos, R. H.; De Castro, E. V. R. *Acta Cryst.* **1998**, *C54*, 517. (f) Moreno-Fuquen, R.; De Castro, E. V. R.; Moreno, M.; De Almeida Santos, R. H.; Montaño, A. M. *Acta Cryst.* **2000**, *C56*, 206.
10. Allen, F. H.; Raithby, P. R.; Shields, G. P.; Taylor, R. *Chem. Commun.* **1998**, 1043.
11. Lommerse, J. P. M.; Taylor, R. *J. Enzyme Inhibition* **1997**, *11*, 223.
12. (a) Leiserowitz, L. *Acta Cryst.* **1976**, *B32*, 775. (b) Leiserowitz, L.; Hagler, A. T. *Proc. Roy. Soc. London* **1983**, *A388*, 133. (c) Aakeroy, C. B.; Seddon, K. R. *Chem. Soc. Rev.* **1993**, 397. (d) Ashton, P. R.; Collins, A. N.; Fyfe, M. C. T.; Menzer, S.; Stoddart, J. F.; Williams, D. J. *Angew. Chem., Int. Ed. Engl.* **1997**, *36*, 735.
13. For references related to the use of graph-set notation, see (a) Etter, M. C.; MacDonald, J. C.; Bernstein, J. *Acta Cryst.* **1990**, *B46*, 256. (b) Bernstein, J.; Davis, R. E.; Shimoni, L.; Chang, N.-L. *Angew. Chem., Int. Ed. Engl.* **1995**, *34*, 1555.
14. Leiserowitz, L.; Nader, F. *Acta Cryst.* **1977**, *B33*, 2719.
15. Etter, M. C. *Acc. Chem. Res.* **1990**, *23*, 120.
16. Bodige, S. G.; Rogers, R. D.; Blackstock, S. C. *Chem. Commun.* **1997**, 1669.

17. Fuquen, R. M.; De A. Santos, R. H.; Lechat, J. R. *Acta Cryst*. **1996**, *C52*, 220.
18. The differential scanning calorimetry results for these cocrystalline solids are available from the author.
19. Morgan, B. P.; Scholtz, J. M.; Ballinger, M. D.; Zipkin, I. D.; Bartlett, P. A. *J. Am. Chem. Soc*. **1991**, *113*, 297.
20. Searle, M. S.; Williams, D. H. *J. Am. Chem. Soc*. **1992**, *114*, 10690.
21. Sheldrick, G. M. SHELXL-93, University of Göttingen.
22. Crystallographic data (excluding structure factors) for the structures in this paper have been deposited with the Cambridge Crystallographic Data Centre as supplementary publication nos. CCDC 135536–135539 for **1·2** to **1·5**, respectively. Copies of the data can be obtained, free of charge, on application to CCDC, 12 Union Road, Cambridge CB2 1EZ, UK (fax: +44-1223-336033 or e-mail: deposit@ccdc.cam.ac.uk).